Resonance Raman Characterization of the Heme Domain of Soluble Guanylate Cyclase†

Johannes P. M. Schelvis,‡ Yunde Zhao,§ Michael A. Marletta,*,§,||,⊥ and Gerald T. Babcock*,‡

Department of Chemistry and LASER Laboratory, Michigan State University, East Lansing, Michigan 48824-1322, and Department of Biological Chemistry, School of Medicine, Howard Hughes Medical Institute, and Interdepartmental Program in Medicinal Chemistry, College of Pharmacy, University of Michigan, Ann Arbor, Michigan 48109-1065

Received June 30, 1998; Revised Manuscript Received September 28, 1998

ABSTRACT: We report the resonance Raman characterization of the heme domain of rat lung soluble guanylate cyclase (sGC) expressed in *Escherichia coli*. Like heterodimeric sGC isolated from bovine lung, the sGC heme domain [β1(1−385)] and its heme ligand mutant H105G(Im) contain a stoichiometric amount of heme, which is five-coordinate, high-spin ferrous in both β1(1−385) and chemically reduced H105G(Im). In the presence of NO, both β1(1−385) and H105G(Im) form a five-coordinate nitrosyl heme complex with a ν(Fe−NO) value of 525 cm^{-1} and a ν(NO) value of 1676 cm^{-1}. For the first time, the Fe−N−O bending mode near 400 cm^{-1} has been identified in a five-coordinate nitrosyl heme complex. Both β1(1−385) and H105G(Im) form a six-coordinate, low-spin complex with CO. We find evidence for two binding conformations of the Fe−CO unit. The conformation that is more prevalent in β1(1−385) has a ν(Fe−CO) value of 478 cm^{-1} and a δ(Fe−C−O) value of 567 cm^{-1}, whereas the dominant conformation in H105G(Im) is characterized by a ν(Fe−CO) value of 495 cm^{-1} and a δ(Fe−C−O) value of 572 cm^{-1}. We propose that in the dominant conformation of H105G(Im)−CO the Fe−CO unit is hydrogen bonded to a distal residue, while this is not the case in β1(1−385). Reexamination of sGC isolated from bovine lung tissue indicates that it also has two binding conformations for CO; the more populated form is not hydrogen-bonded. We propose that the absence of hydrogen-bond formation between a distal residue and exogenous ligands is physiologically relevant in lowering the oxygen affinity of heterodimeric sGC and, therefore, stabilizing the ferrous, active form of the enzyme under aerobic conditions.

Guanylate cyclase catalyzes the conversion of GTP[1] to cGMP and pyrophosphate. The generated cGMP plays an important role in several biological processes, e.g., vasodilation and neurotransmission (*1*−*4*). Two forms of the enzyme are known: particulate guanylate cyclase (pGC) and soluble guanylate cyclase (sGC). The membrane-bound protein, pGC, is activated by ligands such as small peptide hormones, while nitric oxide (NO) regulates the activity of sGC, the only known receptor for NO (*3*−*5*). sGC, isolated from lung tissue, is a heterodimeric hemoprotein that consists of α1 and β1 subunits (*6*−*10*). Both the α1 and the β1 subunits are required for enzymatic activity (*11*, *12*). The catalytic sites are contained within the C-terminal region of the two subunits (*13*, *14*). The heme binding region has been localized to the N-terminal region of the β1 subunit (*15*, *16*). NO activates sGC more than 400-fold over the basal activity, while CO activates sGC only 4−5-fold (*17*). Bound heme is required for both NO and CO activation of sGC (*18*, *19*). NO and CO binding to the sGC heme at the N-terminal region induce a conformational change in the heme pocket (*20*), which activates the enzyme presumably via conformational changes in the catalytic site(s) at the C-terminal region. It has been shown that a five-coordinate nitrosyl complex is formed upon NO coordination to the heme with concomitant cleavage of the bond between the heme iron and the proximal histidine (*21*−*23*). In the case of CO, stimulated activity of sGC is observed with the bond between the heme iron and the proximal histidine apparently intact (*21*, *22*, *24*).

Elucidation of the sGC activation mechanism depends on our understanding of the sGC heme environment and the structural changes induced by NO and CO binding to the sGC heme cofactor. Spectroscopic studies of the activation mechanism require relatively large amounts of enzyme. Although progress is being made in increasing the yield of sGC isolated from bovine lung tissue, overexpression techniques are required to obtain large amounts of protein that will allow different experimental approaches in the study of sGC (de)activation. It is important to establish whether the overexpressed protein has NO-stimulated activity and spectroscopic properties comparable to those of heterodimeric

† The studies were supported by NIH Grant GM25480, the Searle chair endowment fund, and the Howard Hughes Medical Institute.

* To whom correspondence should be addressed.
‡ Michigan State University.
§ Department of Biological Chemistry, University of Michigan.
|| Howard Hughes Medical Institute, University of Michigan.
⊥ College of Pharmacy, University of Michigan.

[1] Abbreviations: β1(1−385), N-terminal fragment of β1 subunit residues 1−385 of sGC; pGC, particulate guanylate cyclase; sGC, soluble guanylate cyclase; cGMP, guanosine 3′,5′-cyclic monophosphate; GTP, guanosine 3′,5′-triphosphate; H105G(Im), β1(1−385) H105G mutant expressed and purified in the presence of imidazole with heme bound; HO, heme oxygenase; Im, imidazole; Mb, myoglobin; *N*-MeIm, *N*-methylimidazole.

10.1021/bi981547h CCC: $15.00
Published on Web 10/28/1998

sGC isolated from tissue. The overexpression of heterodimeric sGC by using transfected baculovirus cells was reported recently, and the reconstituted heme was present as a mixture of five-coordinate, high-spin and six-coordinate, low-spin ferrous complexes (*25*, *26*). The spin and coordination state of the heme in heterodimeric sGC as isolated is still a point of controversy in the literature. The results of Rousseau and co-workers (*26*) are in agreement with an earlier study on heterodimeric sGC isolated from bovine lung (*23*), while our groups and others have reported that heterodimeric sGC from bovine lung contains only a five-coordinate, high-spin ferrous heme (*22*, *27*, *28*).

Recently, we reported the overexpression of a fragment of the β1 subunit [β1(1−385)] of rat lung sGC in *Escherichia coli*, which demonstrated that the heme binding region is in the N terminus of the β1 subunit (*15*). UV−vis spectroscopic studies indicate that β1(1−385) contains a five-coordinate, high-spin ferrous heme (*15*). Through site-directed mutagenesis and spectroscopic approaches, we demonstrated that the heme in sGC is coordinated to the proximal His105 in the β1 subunit (*29*). Mutation of His105 to glycine in β1(1−385) leads to the loss of heme binding to the heme domain. Heme binding to the β1(1−385) H105G mutant [H105G(Im)] was restored by adding imidazole to the media and purification buffers. In the ferrous form, the heme in H105G(Im) is also five-coordinate with imidazole as the proximal ligand. To use these truncated proteins as models for investigating the properties and ligand dynamics of the heme pocket of heterodimeric sGC, it is important to characterize their spectroscopic properties relative to those of heterodimeric sGC. In this paper, we report the resonance Raman characterization of β1(1−385) and H105G(Im) in the ferrous form, and of the complexes with CO and NO. The resonance Raman spectra of these three complexes of the two protein fragments are very similar to those of heterodimeric sGC purified from bovine lung tissue. This result indicates that the heme environment in β1(1−385) closely resembles that of heterodimeric sGC. In the CO complexes of β1(1−385) and H105G(Im), we have observed two conformations of the Fe−CO unit, which we also identified in heterodimeric sGC. We believe that in H105G(Im)−CO the dominant binding conformation of CO is hydrogen-bonded by a distal residue, while this is not the case in β1(1−385)−CO and sGC−CO.

MATERIALS AND METHODS

Sample Preparation. The construction of the β1(1−385) fragment and of H105G(Im) from rat lung cDNA and their purification procedures have been described in detail elsewhere (*15*, *29*). The cDNAs encoding β1(1−206) and β1-(1−345) were cloned in the pET 20b plasmid using *Nde*I−*Bam*HI. Both β1(1−206) and β1(1−345) were expressed in *E. coli* BL21 (DE3pLys) under control of a T7 promotor. The cell culture conditions for expression of these two smaller fragments were the same as those for β1(1−385) as described in ref *15*. Both β1(1−206) and β1(1−345) were purified by a two-step purification procedure (ion exchange and gel filtration) with conditions similar to those for the β1(1−385) purification. All Raman samples were prepared in spinning cells that could be sealed with a septum. Experiments with β1(1−385) in 50 mM Hepes (pH 7.4), 100 mM NaCl, and 5 mM DTT were carried out under an Ar atmosphere. This protein is isolated as a stable five-coordinate, high-spin ferrous complex (*15*, *29*). H105G β1-(1−385) is isolated without any heme present. If expressed and purified in the presence of imidazole [H105G(Im)], it then is isolated with a stoichiometric equivalent of ferric heme (*29*). In the case of H105G(Im), the sample was put under an Ar atmosphere and subsequently reduced with a small amount of dithionite in the presence of 1 mM imidazole. Since β1(1−385) contains a ferrous heme, the CO complex was prepared by simply placing the enzyme under a CO atmosphere. In the case of H105G(Im), the CO complex was obtained by reducing the enzyme with dithionite in the presence of 1 mM imidazole, while the sample was under a CO atmosphere. Finally, the NO complexes of β1(1−385) and H105G(Im) were formed by adding NO gas anaerobically into the headspace of the spinning cell. The $^{13}C^{18}O$ and $^{15}N^{18}O$ isotopes were obtained from Isotech Inc. (Miamisburg, OH). Mass spectroscopic analysis of the nitric oxide isotope showed that it consisted of a mixture of $^{15}N^{16}O$ and $^{15}N^{18}O$. The identification of the NO sensitive vibrations was not affected by this mixture. Both isotopic forms of NO were purified from other nitrogen oxides by passage through saturated KOH.

Resonance Raman Experiments. The resonance Raman spectra of ferrous β1(1−385) and H105G(Im), and the respective CO complexes, were collected with 413.1 nm excitation light from a Kr^+ laser (Coherent K-90). The spectra of the NO complexes were obtained by excitation with the 406.7 nm line from the same laser. Laser powers were typically 5 mW at the samples, except for the CO complexes in which case a power of ≤1 mW was used to prevent CO photolysis. The laser light was focused on the sample by a spherical lens with a focal length of 5.5 cm. The resonance Raman scattering was detected with a spectrometer (Spex 1877 Triplemate) in combination with a liquid nitrogen-cooled CCD detector (EG&G OMA 4, model 1530-CUV-1024S). A spectral slit width of 3 cm^{-1} was used. Accumulation times are indicated in the figure legends. The samples were kept at about 10 °C during the experiments. The resonance Raman spectra were baseline corrected. In the low-frequency region (below 250 cm^{-1}), the rise in the baseline, which is induced by Rayleigh scattering and reflected laser light, was corrected by subtracting either a Gaussian or a monoexponential curve. At the high-frequency side of the spectrum, the baseline was flattened, if necessary, by subtraction of either a straight line or a second-order polynomial. The difference spectra were obtained by normalizing the absolute spectra with respect to heme skeletal vibrations and subsequent subtraction of the heavy isotope spectrum from the natural-abundance isotope spectrum. This procedure was carried out prior to baseline correction of the absolute spectra. The heme vibrational modes were labeled according to ref *30*, and the vibrational modes in the β1(1−385) and H105G(Im) complexes were assigned on the basis of the work with heterodimeric sGC (*22*, *27*).

RESULTS

Ferrous β1(1−385) and H105G(Im). The low- and high-frequency resonance Raman spectra of β1(1−385) are shown in parts a and c of Figure 1, respectively. We used 413 nm excitation to collect the spectra to facilitate comparison with

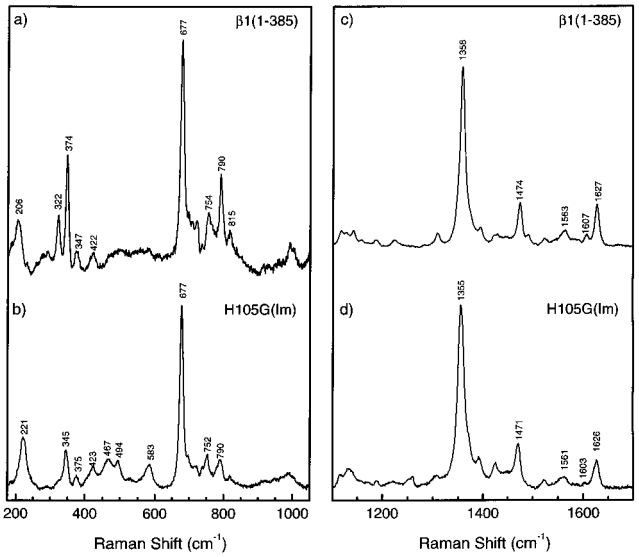

FIGURE 1: Low- and high-frequency resonance Raman spectra of the ferrous forms of β1(1−385) and H105G(Im) obtained with 413.1 nm excitation: (a and c) 80 μM β1(1−385) and (b and d) 50 μM H105G(Im). The accumulation time was 30 min for each of the high-frequency spectra and 60 min for each of the low-frequency spectra. See the text for further experimental conditions.

the resonance Raman spectra of the CO and NO complexes of β1(1−385) and H105G(Im). Also, at this wavelength the presence of any six-coordinate, low-spin ferrous heme would be detected, since such a complex would have an absorption maximum around 425 nm (*31*), and its Raman signal would be enhanced relative to that of a five-coordinate, high-spin ferrous heme. Soret excitation enhances vibrations that give insight into heme structure (*32*−*34*). The oxidation and coordination state of the heme can be determined from the π-electron density marker, ν_4, which reflects the oxidation state of the heme iron, and the spin and coordination state markers, ν_3, ν_2, and ν_{10}, which are sensitive to the core size of the heme macrocycle (*34*). The high-frequency spectrum of β1(1−385) (Figure 1c) is very similar to that of heterodimeric sGC isolated from bovine lung tissue (*22*, *27*). The heme skeletal vibrations ν_2, ν_3, ν_4, and ν_{10} are observed at 1563, 1474, 1358, and 1607 cm^{-1}, respectively. The frequencies of these vibrations indicate that β1(1−385) contains a five-coordinate, high-spin ferrous heme (*33*). The low-frequency spectrum of β1(1−385) collected with 413 nm excitation (Figure 1a) compares very well with that obtained with 431 nm excitation (*29*). The Raman intensities of some vibrations are different for the two excitation wavelengths, reflecting Raman excitation profile effects, but the frequencies are independent of the excitation wavelength. The vibration at 206 cm^{-1} has previously been assigned to the stretching vibration involving the heme iron and the proximal histidine, H105 in the β1 subunit (*29*). This vibration is observed at a slightly lower frequency, 204 cm^{-1}, in heterodimeric sGC (*22*, *27*).

The high-frequency spectrum of the H105G(Im) mutant of β1(1−385) is shown in Figure 1d. The heme skeletal modes ν_2, ν_3, ν_4, and ν_{10} are observed at 1561, 1471, 1355, and 1603 cm^{-1}, respectively. These frequencies are slightly lower than those for β1(1−385). From the frequencies of the skeletal modes, we conclude that reduced H105G(Im) also contains a five-coordinate, high-spin ferrous heme. The low-frequency spectrum of ferrous H105G(Im) (Figure 1b) is very similar to the spectrum of the β1(1−385) fragment except for the Fe−His vibration at 206 cm^{-1} that has been replaced by an Fe−Im vibration at 221 cm^{-1} (*29*). The frequency of this vibration compares well with those observed for other heme proximal ligand mutants (see Table 1). Several high-frequency skeletal vibrational modes and the Fe−ligand vibration of β1(1−385) and H105G(Im) are listed in Table 1 together with those of other proteins and the respective heme proximal ligand mutants.

Table 1: Heme Skeletal Vibrations of Different Isoforms of sGC, Myoglobin (Mb), Heme Oxygenase (HO), and Their Respective Heme Ligand Mutants[a]

	ν_{CC}	ν_{10}	ν_2	ν_3	ν_4	ν(Fe−L)	reference
sGC H105G(Im)	1626	1603	1561	1471	1355	221[d]	this work
sGC β1(1−385)	1627	1607	1563	1474	1358	206[e]	this work
heterodimeric sGC[b]	1626	1606	1562	1471	1358	204[e]	*22*, *27*
heterodimeric sGC[c]	1617	1627	1582	1470/1492	1359	no[f]	*23*, *26*
Mb H93G(Im)	nr[h]	nr	nr	nr	nr	225[d]	*g*
Mb	1618	1607	1563	1471	1357	220[e]	*35*
HO H25A(Im)	nr	nr	nr	nr	nr	225[d]	*42*
HO H25G(Im)	nr	nr	nr	nr	nr	220[d]	*42*
HO	1620	1605	1562	1470	1354	217[e]	*56*

[a] All frequencies are given in cm^{-1}. [b] Heme retained during isolation and purification procedures. [c] Heme reconstituted after isolation and purification procedures. [d] L = imidazole. [e] L = histidine. [f] Not observed. [g] S. Franzen, personal communication. [h] Not reported.

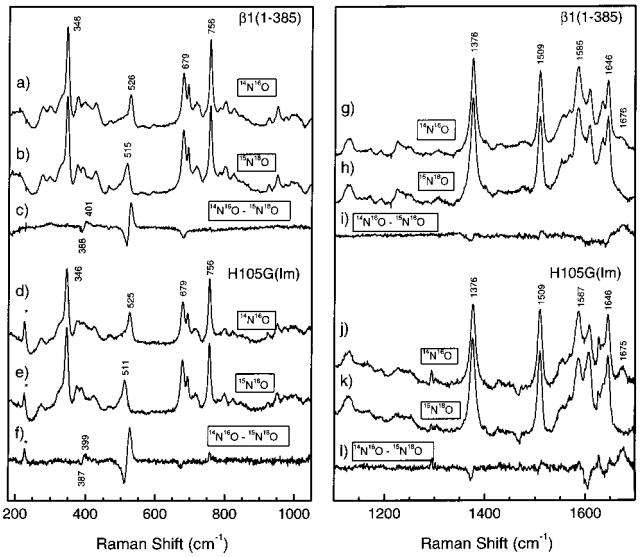

FIGURE 2: Low- and high-frequency resonance Raman spectra of the NO complexes of β1(1−385) and H105G(Im) obtained with 406.7 nm excitation: (a and g) β1(1−385)−$^{14}N^{16}O$, (b and h) β1(1−385)−$^{15}N^{18}O$, (c and i) difference spectra of β1(1−385)−NO ($^{14}N^{16}O$ − $^{15}N^{18}O$), (d and j) H105G−$^{14}N^{16}O$, (e and k) H105G−$^{15}N^{18}O$, and (f and l) difference spectra of H105G−NO ($^{14}N^{16}O$ − $^{15}N^{18}O$). The asterisk in parts d−f indicates a plasma line from the laser. The accumulation time was 30 and 60 min for the high- and low-frequency spectra, respectively. The protein concentration was 50 μM; see the text for further experimental conditions.

Nitrosyl Complexes of β1(1−385) and H105G(Im). The resonance Raman spectra obtained for the nitrosyl complex of β1(1−385) and H105G(Im) (Figure 2) are very similar to those of native, heterodimeric sGC (*22*, *27*). In the high-frequency region (Figure 2g), the β1(1−385) nitrosyl complex has the spectrum characteristic of a five-coordinate

Table 2: Heme Skeletal Vibrations and Vibrational Modes Involving the NO Moiety in Different Isoforms of sGC, Myoglobin (Mb), and Mb H93G(Im)[a]

	ν_{10}	ν_2	ν_3	ν_4	Fe−NO	Fe−N−O	N−O	reference
H105G(Im)	1646	1587	1509	1376	525	399	1675	this work
β1(1−385)	1646	1585	1509	1376	526	401	1676	this work
sGC[b]	1646	1584	1509	1375	525	no[f]	1677	*22*, *27*
sGC[c]	1645	1584	1508	1375	520[d]	no	no	*23*, *26*
Mb H93G(Im)	1651	nr[g]	1509	1376	525[e]	nr	nr	*55*
Mb	1638	1584	1501	1375	554	449	1624	*36*, *45*

[a] All frequencies are given in cm^{-1}. [b] Heme retained during isolation and purification procedures. [c] Heme reconstituted after isolation and purification procedures. [d] Only reported in ref *26*. [e] S. Franzen, personal communication. [f] Not observed. [g] Not reported.

nitrosyl heme (*36*). The skeletal modes ν_2, ν_3, ν_4, and ν_{10} are observed at 1585, 1509, 1376, and 1646 cm^{-1}, respectively. The ν(NO) frequency was determined by measuring the resonance Raman spectrum of the $^{15}N^{18}O$ complex of β1(1−385) (Figure 2h). One isotope sensitive vibration was detected in the high-frequency difference spectrum at 1676 cm^{-1} (Figure 2i). We assign this vibration to ν(NO). In the low-frequency spectrum of β1(1−385)−NO, we detect two isotope sensitive vibrations (Figure 2a−c). We assign the band at 526 cm^{-1} to the Fe−NO stretching vibration. The band near 401 cm^{-1} most likely arises from the Fe−N−O bending mode that has not been observed before in sGC−NO or any other five-coordinate NO−heme complex.

The results for the ferrous nitrosyl complex of H105G(Im) are very similar to those of β1(1−385). In the high-frequency spectrum (Figure 2j−l), the skeletal vibrations ν_2, ν_3, ν_4, and ν_{10} are observed at 1587, 1509, 1376, and 1646 cm^{-1}, respectively. From these results, we conclude that H105G(Im) also forms a five-coordinate complex with NO. In the isotope difference spectrum (Figure 2l), the NO stretching vibration was detected at 1675 cm^{-1}. In the low-frequency region (Figure 2d−f), the Fe−NO stretching vibration was observed at 525 cm^{-1} and the Fe−N−O bending mode around 399 cm^{-1}. The results for the nitrosyl complexes of β1(1−385) and H105G(Im) compare very well with those of heterodimeric sGC (*22*, *27*). The high-frequency skeletal vibrations and the modes involving the NO moiety of β1(1−385)−NO and H105G−NO are listed in Table 2 together with those of myoglobin (Mb) and its heme proximal ligand mutant Mb H93G(Im).

Carbonyl Complexes of β1(1−385) and H105G(Im). The resonance Raman spectra of β1(1−385)−CO and ferrous H105G(Im)−CO are shown in Figure 3. The high-frequency spectrum of β1(1−385)−CO (Figure 3g) has a ν_4 at 1372 cm^{-1}; the absence of a low-frequency shoulder indicates that no photolysis product is observed. Following the assignments for the CO complex of heterodimeric sGC, we attribute the bands at 1496 and 1582 cm^{-1} to the ν_3 and ν_2 vibrational modes, respectively (*22*). The ν_{10} vibrational mode is expected around 1620 cm^{-1} (*33*). Overlap with the vinyl stretching vibration (ν_{CC}) near 1629 cm^{-1}, however, hinders the assignment of the ν_{10} vibration.

The low-frequency spectra of β1(1−385)−$^{12}C^{16}O$ and β1(1−385)−$^{13}C^{18}O$ and the difference spectrum are shown in parts a−c of Figure 3, respectively. Enlargements of the difference spectra are shown in Figure 4b. We observed five isotope sensitive bands. The first two bands at 478 cm^{-1} and around 495 cm^{-1} are assigned to the Fe−CO stretching vibration [ν(Fe−CO)] that most likely arise from two different conformations of the Fe−CO unit. We assign the

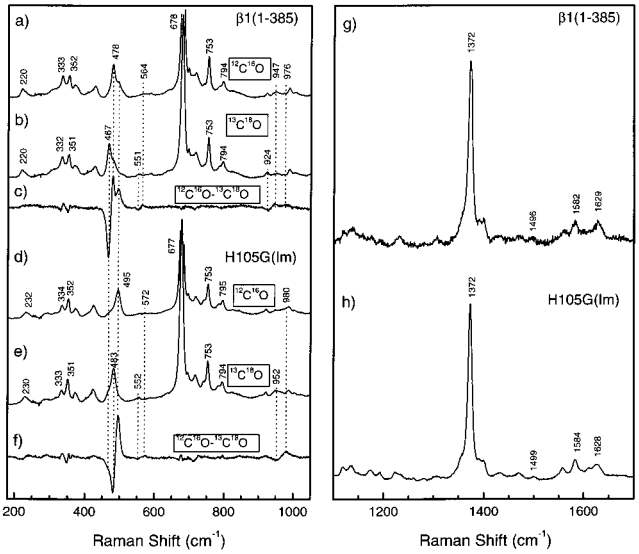

FIGURE 3: Low- and high-frequency resonance Raman spectra of the CO complexes of β1(1−385) and H105G(Im) obtained with 413.1 nm excitation: (a and g) β1(1−385)−$^{12}C^{16}O$, (b) β1(1−385)−$^{13}C^{18}O$, (c) difference spectrum of β1(1−385)−CO ($^{12}C^{16}O$ − $^{13}C^{18}O$), (d and h) H105G(Im)−$^{12}C^{16}O$, (e) H105G(Im)−$^{13}C^{18}O$, and (f) difference spectrum of H105G(Im)−CO ($^{12}C^{16}O$ − $^{13}C^{18}O$). The accumulation time was 30 and 90 min for the high- and low-frequency spectra, respectively. The protein concentration was 25 μM; see the text for further experimental conditions.

isotope sensitive band at 564 cm^{-1} to the Fe−C−O bending mode [δ(Fe−C−O)]. The isotope sensitive bands at 947 and 976 cm^{-1} are overtone vibrations of the two ν(Fe−CO) modes. The frequencies of these overtone vibrations are less than twice their fundamental frequencies due to anharmonicity of their potential energy curves. Overtone vibrations of ν(Fe−CO) have been observed before in other heme proteins (*37*).

In the case of H105G(Im)−CO, CO photolysis has been minimized. The high-frequency spectrum (Figure 3h) shows a very weak shoulder around 1355 cm^{-1} on the ν_4 vibration at 1372 cm^{-1} indicative of a small amount of photolysis product. However, the main features in the spectrum arise from the H105G(Im)−CO complex, and we assign the vibrations at 1584 and 1499 cm^{-1} to the ν_2 and ν_3 vibrational modes, respectively (*22*). The ν_{CC} mode is observed at 1628 cm^{-1}, but an unambiguous assignment of the ν_{10} vibration was not possible.

The low-frequency spectra of H105G−$^{12}C^{16}O$ and H105G−$^{13}C^{18}O$ and the difference spectrum are shown in parts d−f of Figure 3, respectively. An enlargement of several regions of the difference spectrum is shown in Figure 4c. We identified four isotope sensitive bands. The band at 495 cm^{-1} is attributed to the ν(Fe−CO) mode. It is interesting that

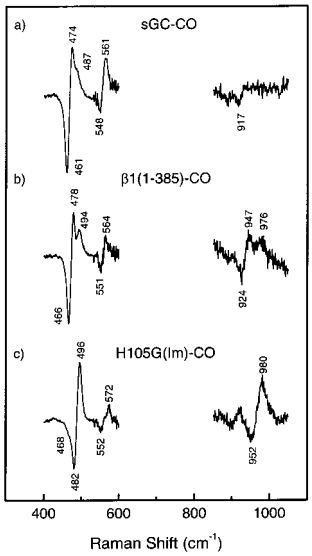

FIGURE 4: Enlargements (5 times larger, except for the 400−540 cm^{-1} region) of the $^{12}C^{16}O - {}^{13}C^{18}O$ difference spectra of heterodimeric sGC−CO (a, adapted from ref *22*), β1(1−385)−CO (b, from Figure 3c), and H105G(Im)−CO (c, from Figure 3f). The peak positions in the difference spectra may vary slightly from those of the absolute spectra due to the subtraction.

this vibration coincides with one of the two ν(Fe−CO) vibrations observed in β1(1−385)−CO. On closer inspection of the difference spectrum, a second ν(Fe−CO) can be observed in the difference spectrum (Figure 4c) near 468 cm^{-1}. This is the low-frequency ν(Fe−$^{13}C^{18}O$). Its $^{12}C^{16}O$ counterpart is expected near 478 cm^{-1}, the low-frequency ν(Fe−CO) mode in β1(1−385)−CO (Figure 4b). Apparently, both ν(Fe−CO) vibrations are also present in H105G(Im)−CO, but their intensity ratio has changed in favor of the 495 cm^{-1} form. We assign the isotope sensitive band at 572 cm^{-1} to δ(Fe−C−O). We also observed an isotope sensitive vibration around 980 cm^{-1}, which we assign to the overtone vibration of ν(Fe−CO), the 495 cm^{-1} mode. The features below 400 cm^{-1} in the difference spectra of β1(1−385)−CO (Figure 3c) and H105G(Im)−CO (Figure 3f) are very reproducible, but no CO isotope sensitive vibrations are expected in that frequency region. The origin of these isotope sensitive shifts remains unclear, but may reflect a slight mixing of Fe−CO vibrations with heme skeletal modes. Table 3 contains a list of several high-frequency skeletal vibrational modes and the vibrations involving the CO moiety of β1(1−385)−CO and H105G(Im)−CO together with those of Mb−CO and Mb H93G(Im)−CO.

In Figure 5, we show the resonance Raman spectra of the CO complexes of four β1 subunit fragments. The fraction of CO complex with ν(Fe−CO) at 495 cm^{-1} seems to increase with decreasing size of the heme domain, while it is the largest in the case of H105G(Im)−CO. The spectra of β1(1−206)−CO and β1(1−345)−CO are different from those of β1(1−385)−CO and H105G(Im)−CO in the region from 300 to 450 cm^{-1}. These differences are most likely due to a less rigid protein structure in the smaller heme domain fragments, which may result in slightly changed heme geometry and heme−protein interactions.

DISCUSSION

Ferrous Form of β1(1−385) and H105G(Im). The resonance Raman spectra in Figure 1 show that β1(1−385) of rat lung sGC is almost identical to that of the heterodimeric sGC isolated from bovine lung. In both cases, the protein contains a five-coordinate, high-spin ferrous heme, and the Fe−His stretching vibration [ν(Fe−His)] occurs at an unusually low frequency. The 2 cm^{-1} difference in ν(Fe−His) values between β1(1−385) and heterodimeric sGC is reproducible and may indicate a minor perturbation at the proximal side of the heme pocket caused by the absence of the α1 subunit or of the C-terminal portion of the β1 subunit. Alternatively, it may be due to minor differences between rat lung and bovine lung sGC (*40*, *41*). We conclude that the heme pocket has not been significantly perturbed by the truncation of the β1 subunit and that β1(1−385) serves as a good model for the study of the heme pocket of heterodimeric sGC.

The high-frequency resonance Raman spectrum of dithionite-reduced H105G(Im) is similar to that of heterodimeric sGC and β1(1−385) and characteristic of a five-coordinate, high-spin ferrous heme (Figure 1d). As in the case of β1(1−385), no six-coordinate, low-spin ferrous heme is observed. In the low-frequency resonance Raman spectrum, the Fe−Im stretching vibration occurs at 221 cm^{-1} (Figure 1b). Although ν(Fe−His) in heterodimeric sGC and in β1(1−385) is significantly lower than that observed in other proteins, the frequency of ν(Fe−Im) in H105G(Im) compares well with that observed for the heme proximal ligand mutants of these other proteins (Table 1). The low frequency of ν(Fe−His) in heterodimeric sGC was attributed to the lack of hydrogen bonding to the His N_δ proton (*22*). The relatively large increase of ν(Fe−Im) in H105G(Im) [$\Delta\nu_{His\rightarrow Im} = \nu$(Fe−His) − ν(Fe−Im) = 15 cm^{-1}] when compared to Mb and heme oxygenase (HO) mutants [$\Delta\nu_{His\rightarrow Im} = 5$ and 3−8 cm^{-1}, respectively] indicates that the low ν(Fe−His) in sGC and in β1(1−385) may be partially induced by strain from the protein.

The Fe−Im stretching vibration in H105G(Im) is observed at almost the same frequency as that in HO H25G(Im) (*42*). In the case of HO, it was shown that the proximal residue introduced by mutagenesis can affect the Fe−Im stretching vibration. In HO H25A(Im), ν(Fe−Im) was observed at 225 cm^{-1}, while in H25G(Im), ν(Fe−Im) was observed at 220 cm^{-1}. This behavior was attributed to different interactions between the amino acid side chains and the imidazole ring. In the case of Mb H93G(Im), imidazole is hydrogen-bonded to the S92 hydroxyl and the carboxylate of the heme propionate group (*43*), which probably explains the higher ν(Fe−Im) frequency observed in Mb H93G(Im)[2] (*44*). From these observations, we conclude that the imidazole in H105G(Im) is neither strongly hydrogen-bonded nor experiencing much steric hindrance in the proximal heme pocket.

Our results clearly show that β1(1−385) from rat lung sGC cDNA overexpressed in *E. coli* is isolated with a five-coordinate, high-spin ferrous heme. Also, H105G(Im) forms a five-coordinate, high-spin ferrous heme on reduction. Excitation of the samples at 413.1 nm, which would enhance Raman scattering from six-coordinate, low-spin ferrous heme over its five-coordinate, high-spin counterpart, did not reveal any evidence of six-coordinate, low-spin heme. This is in agreement with previous results with heterodimeric sGC

[2] S. Franzen, personal communication.

Table 3: Heme Skeletal Vibrations and Vibrational Modes Involving the CO Moiety in Different Isoforms of sGC, Myoglobin (Mb), and Mb H93G(Im)[a]

	ν_{10}	ν_2	ν_3	ν_4	Fe−CO[f]	Fe−C−O	C−O	reference
H105G(Im)	nd[d]	1584	1499	1372	478/**495**	571	nd	this work
β1(1−385)	nd	1582	1496	1373	**478**/494	564	nd	this work
sGC[b]	1629	1583	1500	1371	**472**/487	562	1987	*22*, *27*, *48*
sGC[c]	1627	1582	1497	1371	497	574	1959	*23*, *26*
Mb H93G(Im)	nr[e]	nr	nr	nr	512[g]	nr	1945	*39*
Mb	1637	1587	1498	1372	512	577	1944	*38*

[a] All frequencies are given in cm^{-1}. [b] Heme retained during isolation and purification procedures. [c] Heme reconstituted after isolation and purification procedures. [d] Not determined. [e] Not reported. [f] The frequency in bold indicates the dominant conformation; the frequencies ν(Fe−CO) in the nondominant conformations were estimated from the various absolute and difference spectra with an accuracy of about 1 cm^{-1}. [g] S. Franzen, personal communication.

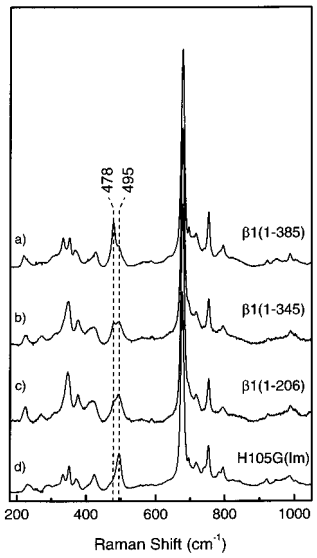

FIGURE 5: Low-frequency resonance Raman spectra of the CO complexes of different heme domain fragments obtained with 413.1 nm excitation: (a) β1(1−385)−CO, (b) β1(1−345)−CO, (c) β1-(1−206)−CO, and (d) H105G(Im)−CO.

isolated from bovine lung, which was shown to contain a five-coordinate, high-spin ferrous heme (*22*, *27*). Our results differ from studies performed on heterodimeric sGC into which the heme cofactor was reconstituted after isolation (*23*, *26*). In that work, the heme cofactor in sGC is present as a mixture of five-coordinate, high-spin and six-coordinate, low-spin ferrous heme. The cause of this difference is not clear but may be due to reconstitution or heterogeneity related to different isolation procedures and enzyme tissue sources.

Nitrosyl Complex of β1(1−385) and H105G(Im). Except for the isotope sensitive vibration near 400 cm^{-1}, the resonance Raman spectra of β1(1−385)−NO and H105G−NO are similar to that of heterodimeric sGC−NO. This 400 cm^{-1} vibration is the lowest NO sensitive vibration reported for heme proteins. It is about 50 cm^{-1} lower in frequency than the lowest vibration involving NO that is observed in six-coordinate nitrosyl complexes. In those complexes, two low-frequency isotope sensitive vibrations have been detected, a weak band around 450 cm^{-1} and a stronger band near 550 cm^{-1} (*45*, *46*). Hu and Kincaid showed that, in six-coordinate nitrosyl complexes, the stretching and bending modes involving the NO moiety show considerable mixing (*45*). The vibration around 550 cm^{-1} has more stretching character, while that near 450 cm^{-1} has a greater bending contribution. Since the geometry of the bound NO in five-coordinate nitrosyl complexes is similar to that in the six-coordinate species (*47*), we expect that ν(Fe−NO) and δ(Fe−N−O) are also strongly mixed in five-coordinate nitrosyl complexes. Therefore, we attribute the vibration near 400 cm^{-1} in the five-coordinate NO complex of β1(1−385) and of H105G(Im) to the normal mode that has more δ(Fe−N−O) character.

At first glance, it seems remarkable that ν(Fe−NO) in the three isoforms of sGC is observed at the same frequency as that of five-coordinate Mb H93G−NO (Table 2), as the distal pockets of sGC and Mb are thought to have different polarities (*22*, *48*). Earlier work has shown that both the proximal ligand and the environment of the distal heme pocket influence the extent of the Fe $d_\pi \rightarrow$ ligand π^* back-donation (*49*−*51*). In the case of NO, ν(NO) was shown to be sensitive to environmental effects near the ligand binding site in distal pocket mutants of myoglobin (*52*). Therefore, one would expect that ν(NO) and ν(Fe−NO) would respond to back-donation in a manner similar to that of their CO counterparts. However, this is not supported by data in the literature. In six-coordinate nitrosyl complexes of heme proteins, ν(Fe−NO) has been reported to be in a very narrow range from 554 to 558 cm^{-1} (*45*, *46*). The bending mode has been observed in a similar narrow range from 446 to 453 cm^{-1}. The NO stretching mode, however, shows substantial variation. In the case of Hb and Mb, ν(NO) = 1624 and 1622 cm^{-1}, respectively, while in cytochrome P450$_{cam}$, ν(NO) = 1591 cm^{-1} (*45*). It is known that P450s display a different π-electron back-donation correlation than Hb and Mb because of the proximal ligand (*53*), which is a cysteine instead of a histidine. In the case of CO, however, this affects both ν(CO) and ν(Fe−CO). In the case of NO, the change observed in ν(NO) in cytochrome P450$_{cam}$ relative to that of Mb is not coupled to a change in ν(Fe−NO). We propose that the extensive mixing of δ(Fe−N−O) and ν-(Fe−NO) obscures the effect of π-electron back-donation in ν(Fe−NO) but that ν(NO) remains responsive to this phenomenon. Analogous to ν(CO), ν(NO) is expected at a lower frequency in Mb H93G−NO than in β1(1−385)−NO, H105G−NO, and the nitrosyl complex of heterodimeric sGC. If this were the case, the weak NO stretching vibration will be hidden under the strong skeletal vibrational modes in the 1600−1650 cm^{-1} region. A similar circumstance may hold for heme-reconstituted sGC, since ν(NO) has not been observed in these preparations. The model above may also explain the observation by Kitagawa and co-workers that two NO stretching vibrations are observed in heterodimeric sGC in the presence of GTP and cGMP, but only one ν-(Fe−NO) (*27*).

Carbonyl Complex of β1(1−385) and H105G(Im). The resonance Raman spectra of the CO complexes of β1(1−385) and H105G(Im) are very similar to those of heterodimeric sGC, and are indicative of a six-coordinate, low-spin heme (Figure 3). In the low-frequency region, there are a few differences between β1(1−385)−CO and H105G(Im)−CO. The isotopic labeling of CO indicates that these differences are due to vibrations involving the CO moiety. In β1(1−385)−CO, we detected two Fe−CO stretching vibrations: an intense one at 478 cm^{-1} and a weaker one near 495 cm^{-1}. The same Fe−CO vibrations are present in H105G(Im)−CO, but now the 495 cm^{-1} mode is intense and the 478 cm^{-1} vibration weak. In the CO complex of heterodimeric sGC, only one ν(Fe−CO) has been reported at 472 cm^{-1} (*22*, *27*). The shape of this Raman band, however, is very similar to that in β1(1−385)−CO, that is, an intense peak with a shoulder to the high-frequency side. Reexamination[3] of the data for the CO complex of heterodimeric sGC reveals that in this case there are two Fe−CO stretching vibrations as well, an intense mode at 472 cm^{-1} and a weaker one at about 487 cm^{-1} (Figure 4a). Since two Fe−CO stretching vibrations are also present in heterodimeric sGC, we conclude that two Fe−CO conformations are present in heterodimeric sGC and that this behavior is not strictly a property of the β1 fragment. The Fe−CO vibrations in β1(1−385)−CO and H105G(Im)−CO are detected at frequencies 6−7 cm^{-1} higher than those in heterodimeric sGC. This difference may be caused by a slightly different conformation of the heme pocket or, alternatively, by small differences between bovine and rat lung sGC (*40*, *41*). We also detected δ(Fe−C−O) in β1(1−385)−CO and H105G(Im)−CO at 564 and 572 cm^{-1}, respectively. Since a ν(Fe−CO) of 478 cm^{-1} is dominant in β1(1−385)−CO, we assign a δ(Fe−C−O) of 564 cm^{-1} to this conformation. For the same reason, we assign a δ(Fe−C−O) of 572 cm^{-1} to the dominant conformation in H105G(Im)−CO with a ν(Fe−CO) of 495 cm^{-1}.

The CO isotope sensitive vibrations in the 950−1000 cm^{-1} region can be assigned to the first overtone, ν_{over}, of the Fe−CO stretching vibrations. From the frequencies of the fundamental and overtone Fe−CO vibration, we can calculate the anharmonicity of the potential energy curve of this vibration (*37*). In β1(1−385), two positive bands can be distinguished at about 947 cm^{-1} and near 976 cm^{-1}, while one negative peak due to the heavy isotope is detected at about 924 cm^{-1}. These three overtone vibrations correspond to ν(Fe−CO) at 495, 478, and 466 cm^{-1}, respectively. In H105G(Im)−CO, the overtone vibration of ν(Fe−CO) is observed at 980 cm^{-1}, while the mode due to the heavy isotope of CO is present at 952 cm^{-1}. These overtone vibrations correspond to ν(Fe−CO) at 495 and 482 cm^{-1}, respectively. From the two data sets, we calculate an anharmonicity $2\omega_e\chi_e$ of 8−9 cm^{-1} for the conformation with a ν(Fe−CO) of 478 cm^{-1} and a $2\omega_e\chi_e$ of 10−12 cm^{-1} for the conformation with a ν(Fe−CO) of 495 cm^{-1}. Since the positions of the overtone vibrations are determined from the isotope difference spectra, there may be some uncertainty in the overtone frequencies, which precludes a more detailed interpretation of the calculated anharmonicity values. However, the anharmonicity values are in the range of those observed for other heme proteins (*37*).

Two Conformations of the CO Complex. We classify the two conformations of the CO complex of β1(1−385) as follows. Conformation I is characterized by a ν(Fe−CO) of 478 cm^{-1}, a δ(Fe−C−O) of 564 cm^{-1}, a ν_{over} of 947 cm^{-1}, and a $2\omega_e\chi_e$ of 8−9 cm^{-1}, while conformation II is characterized by a ν(Fe−CO) of 495 cm^{-1}, a δ(Fe−C−O) of 572 cm^{-1}, a ν_{over} of 976−980 cm^{-1}, and a $2\omega_e\chi_e$ of 10−12 cm^{-1}. The change from conformation I to conformation II in the case of H105G(Im)−CO may be induced by the presence of imidazole in the sample. In smaller fragments of the β1 subunit [β1(1−345) and β1(1−206)], however, we observe equal populations of conformations I and II in the CO complexes (see Figure 5). In those preparations, no imidazole was present. Therefore, we can exclude that a direct interaction between imidazole and bound CO controls the change from conformation I to conformation II. We also exclude the effect of the change in chemical properties of the proximal ligand on the Fe−CO vibration, i.e., histidine versus imidazole, because substitution of imidazole with *N*-methylimidazole in H105G changed neither ν(Fe−CO) nor the population ratios of the two conformations (J. P. M. Schelvis, Y. Zhao, M. A. Marletta, and G. T. Babcock, unpublished results).

Because we can eliminate a proximal ligation explanation for rationalizing conformation I versus II behavior, an attractive model is one that invokes variation in the extent to which formation of a hydrogen bond between the CO moiety and a distal residue can occur. The frequency difference between the two Fe−CO stretching vibrations for the two conformations is 17 cm^{-1}. This difference is very similar to that observed for myoglobin and its distal pocket mutant (*54*). In that case, ν(Fe−CO) is observed at 510 and 491 cm^{-1} in the presence and absence, respectively, of a hydrogen bond between CO and a distal histidine. This indicates that hydrogen bonding to the CO moiety by a distal residue may be the difference between the two conformations of the Fe−CO unit in β1(1−385)−CO and H105G(Im)−CO. Although imidazole is ligated at the proximal side of the heme in H105G(Im), there is little or no strain from the protein (see above), and the same may be true in the case of β1(1−206) and β1(1−345), in which deletion of additional amino acid residues with respect to β1(1−385) may have resulted in less strain from the protein at the proximal side. Thus, the heme−CO moiety may be more pliable in terms of its distal pocket interactions, which allows hydrogen bond formation between CO and a distal residue. In this model, in heterodimeric sGC, in which the heme is retained during the purification procedure, the Fe−CO unit occupies mainly conformation I, the non-hydrogen-bonded conformation. To date, we have not been able to perform a detailed pH dependence study of ν(Fe−CO), since both β1(1−385) and H105G(Im) are stable only in a small pH range, i.e., pH 7−9.

Physiological Relevance of the Hydrogen Bond. It has been shown that NO reacts fast with oxyhemoglobin and oxymyoglobin to form methemoglobin and metmyoglobin, respectively (*57*, *58*). In the case of sGC, such a reaction

[3] The low-frequency resonance Raman spectra of sGC−$^{12}C^{16}O$ and of sGC−$^{13}C^{18}O$ (Figure 2b, bottom and top, respectively, from ref *22*) were normalized on the 676 cm^{-1} vibration. Subsequently, the spectrum of the heavy CO isotope was subtracted from that with natural abundance CO.

would lead to the formation of nitrate and the ferric form of the enzyme, which has only basal activity (*59*). Therefore, it is important that the heme cofactor in the enzyme remains ferrous under physiological conditions, i.e., in the presence of oxygen. Indeed, both heterodimeric sGC and β1(1−385) contain a stable five-coordinate, high-spin ferrous heme under aerobic conditions (*15*, *22*, *27*−*29*). sGC has an extremely low oxygen affinity, and both the polarity of the distal heme pocket and the relatively weak Fe−His bond have been considered to lower the oxygen affinity of sGC (*22*, *29*, *48*). However, H105G(Im) is sensitive to oxygen, and under aerobic conditions, this protein contains a ferric heme (*29*). We assume that the distal pocket of H105G(Im) is the same as that of β1(1−385), and the only structural differences between these two proteins are the proximal heme ligand and the possibility of hydrogen bond formation with exogenous ligands in H105G(Im). It has been shown that the relative strength of the Fe−His bond affects the oxygen reactivity in heme proteins, although a clear trend may be obscured by effects from the distal heme pocket (*60*). Therefore, it is likely that the change in proximal ligand from histidine to imidazole induces a change in oxygen sensitivity in H105G(Im) (*29*). In myoglobin, it has been shown that the oxygen affinity increases by more than 300-fold upon hydrogen bond formation between the distal histidine and the bound oxygen molecule (*61*). Therefore, we propose that the possibility of hydrogen bond formation between a distal residue and exogenous ligands in H105G(Im) increases the oxygen sensitivity of H105G(Im) with respect to heterodimeric sGC and β1(1−385). We conclude that in addition to the relatively weak Fe−His bond and relatively negative polarity of the distal heme pocket (*22*, *29*, *48*), the lack of hydrogen bond formation between a distal residue and oxygen in heterodimeric sGC may significantly contribute to the stability of the enzyme under physiological conditions.

ACKNOWLEDGMENT

We thank Dr. Stefan Franzen for discussing his results and sending his manuscript prior to publication.

REFERENCES

1. Bredt, D. S., and Snyder, S. H. (1994) *Annu. Rev. Biochem. 63*, 175−195.
2. Waldman, S. A., and Murad, F. (1987) *Pharmacol. Rev. 39*, 163−196.
3. Garbers, D. L., and Lowe, D. G. (1994) *J. Biol. Chem. 269*, 30741−30744.
4. Wong, S. K.-F., and Garbers, D. L. (1992) *J. Clin. Invest. 90*, 299−305.
5. Arnold, W. P., Mittal, C. K., Katsuki, S., and Murad, F. (1977) *Proc. Natl. Acad. Sci. U.S.A. 74*, 3203−3207.
6. Garbers, D. L. (1979) *J. Biol. Chem. 254*, 240−243.
7. Gerzer, R., Böhme, E., Hofmann, F., and Schultz, G. (1981) *FEBS Lett. 132*, 71−74.
8. Kamisaki, Y., Saheki, S., Nakane, M., Palmieri, J. A., Kuno, T., Chang, B. Y., Waldman, S. A., and Murad, F. (1986) *J. Biol. Chem. 261*, 7236−7241.
9. Mulsch, A., and Gerzer, R. (1991) *Methods Enzymol. 195*, 377−383.
10. Stone, J. R., and Marletta, M. A. (1994) *Biochemistry 33*, 5636−5640.
11. Harteneck, C., Koesling, D., Soling, A., Schultz, G., and Böhme, E. (1990) *FEBS Lett. 272*, 221−223.
12. Buechler, W. A., Nakane, M., and Murad, F. (1991) *Biochem. Biophys. Res. Commun. 174*, 351−357.
13. Foerster, J., Harteneck, C., Malkewitz, J., Schultz, G., and Koesling, D. (1996*) Eur. J. Biochem. 240*, 380−386.
14. Wedel, B., Harteneck, C., Foerster, J., Friebe, A., Schultz, G., and Koesling, D. (1995) *J. Biol. Chem. 270*, 24871−24875.
15. Zhao, Y., and Marletta, M. A. (1997) *Biochemistry 36*, 15959−15964.
16. Friebe, A., Wedel, B., Harteneck, C., Foerster, J., and Koesling, D. (1997) *Biochemistry 36*, 1194−1198.
17. Stone, J. R., and Marletta, M. A. (1995) *Biochemistry 34*, 14668−14674.
18. Ignarro, L. J., Degnan, J. N., Baricos, W. H., Kadowitz, P. J., and Wolin, M. S. (1982) *Biochim. Biophys. Acta 718*, 49−59.
19. Ignarro, L. J., Wood, K. S., and Wolin, M. S. (1982) *Proc. Natl. Acad. Sci. U.S.A. 79*, 2870−2873.
20. Zhao, Y., Hoganson, C. W., Babcock, G. T., and Marletta, M. A. (1998) *Biochemistry 37*, 12458−12464.
21. Stone, J. R., and Marletta, M. A. (1994) *Biochemistry 33*, 5636−5640.
22. Deinum, G., Stone, J. R., Babcock, G. T., and Marletta, M. A. (1996) *Biochemistry 35*, 1540−1547.
23. Yu, A. E., Hu, S., Spiro, T. G., and Burstyn, J. N. (1994) *J. Am. Chem. Soc. 116*, 4117−4118.
24. Friebe, A., and Koesling, D. (1998) *Mol. Pharmacol. 53*, 123−127.
25. Gupta, G., Kim, J., Yang, L., Sturley, S. L., and Danziger, R. S. (1997) *Protein Expression Purif. 10*, 325−330.
26. Fan, B., Gupta, G., Danziger, R. S., Friedman, J., and Rousseau, D. L. (1998) *Biochemistry 37*, 1178−1184.
27. Tomita, T., Ogura, T., Tsuyama, S., Imai, Y., and Kitagawa, T. (1997) *Biochemistry 36*, 10155−10160.
28. Humbert, P., Niroomand, F., Fischer, G., Mayer, B., Koesling, D., Hinsch, K. D., Gausepohl, H., Frank, R., Schultz, G., and Bohme, E. (1990) *Eur. J. Biochem. 190*, 273−278.
29. Zhao, Y., Schelvis, J. P. M., Babcock, G. T., and Marletta, M. A. (1998) *Biochemistry 37*, 4502−4509.
30. Abe, M., Kitagawa, T., and Kyogoku, Y. (1978) *J. Chem. Phys. 69*, 4526−4534.
31. Burstyn, J. N., Yu, A. E., Dierks, E. A., Hawkins, B. K., and Dawson, J. H. (1995) *Biochemistry 34*, 5896−5903.
32. Callahan, P. M., and Babcock, G. T. (1981) *Biochemistry 20*, 952−958.
33. Choi, S., Lee, J. J., Wei, Y. H., and Spiro, T. G. (1983) *J. Am. Chem. Soc. 105*, 3692−3707.
34. Spiro, T. G., and Li, X.-Y. (1988) in *Biological Applications of Raman Spectroscopy* (Spiro, T. G., Ed.) Vol. 3, pp 1−37, Wiley, New York.
35. Choi, S., Spiro, T. G., Langry, K. C., Smith, K. M., Budd, D. L., and La Mar, G. N. (1982) *J. Am. Chem. Soc. 104*, 4345−4351.
36. Tsubaki, M., and Yu, N.-T. (1982) *Biochemistry 21*, 1140−1144.
37. Wang, J., Takahashi, S., and Rousseau, D. L. (1995) *Proc. Natl. Acad. Sci. U.S.A. 92*, 9402−9406.
38. Tsubaki, M., Srivastava, R. B., and Yu, N.-T. (1982) *Biochemistry 21*, 1132.
39. Decatur, S. M., DePillis, G. D., and Boxer, S. G. (1996) *Biochemistry 35*, 3925−3932.
40. Nakane, M., Saheki, S., Kuno, T., Ishii, K., and Murad, F. (1988) *Biochem. Biophys. Res. Commun. 157*, 1139−1147.
41. Koesling, D., Herz, J., Gausepohl, H., Niroomand, F., Hinsch, K. D., Mulsch, A., Bohme, E., Schultz, G., and Frank, R. (1988) *FEBS Lett. 239*, 29−34.
42. Sun, J., Loehr, T. M., Wilks, A., and Ortiz de Montellano, P. R. (1996) in *XVth International Conference on Raman Spectroscopy* (Asher, S. A., and Stein, P. B., Eds.) pp 464−465, Wiley, New York.
43. Barrick, D. (1994) *Biochemistry 33*, 6546−6554.
44. Teraoka, J., and Kitagawa, T. (1981) *J. Biol. Chem. 256*, 3969−3977.
45. Hu, S., and Kincaid, J. R. (1991) *J. Am. Chem. Soc. 113*, 9760−9766.

46. Lukat-Rodgers, G. S., and Rodgers, K. R. (1997) *Biochemistry 36*, 4178−4187.
47. Rovira, C., Kunc, K., Hutter, J., Ballone, P., and Parrinello, M. (1997) *J. Phys. Chem. A 101*, 8914−8925.
48. Kim, S., Deinum, G., Gardner, M. T., Marletta, M. A., and Babcock, G. T. (1996) *J. Am. Chem. Soc. 118*, 8769−8770.
49. Li, X.-Y., and Spiro, T. G. (1988) *J. Am. Chem. Soc. 110*, 6024−6033.
50. Lin, S.-H., Yu, N.-T., Tame, J., Shih, D., Renaud, J.-P., Pagnier, J., and Nagai, K. (1990) *Biochemistry 29*, 5562−5566.
51. Kerr, E. A., Mackin, H. C., and Yu, N.-T. (1983) *Biochemistry 22*, 4373−4379.
52. Vogel, K. M., Dou, Y., Ikeda-Saito, M., and Spiro, T. G. (1996) in *XVth International Conference on Raman Spectroscopy* (Asher, S. A., and Stein, P. B., Eds.) pp 450−451, Wiley, New York.
53. Yu, N.-T., and Kerr, E. A. (1988) in *Biological Applications of Raman Spectroscopy* (Spiro, T. G., Ed.) Vol. 3, pp 39−95, Wiley, New York.
54. Unno, M., Christian, J. F., Olson, J. S., Sage, J. T., and Champion, P. M. (1998) *J. Am. Chem. Soc. 120*, 2670−2671.
55. Decatur, S. M., Franzen, S., DePillis, G. D., Dyer, R. B., Woodruff, W. H., and Boxer, S. G. (1996) *Biochemistry 35*, 4939−4944.
56. Sun, J., Wilks, A., Ortiz de Montellano, P. R., and Loehr, T. M. (1993) *Biochemistry 32*, 14151−14157.
57. Doyle, M. P., and Hoekstra, J. W. (1981) *J. Inorg. Biochem. 14*, 351−358.
58. Hevel, J. M., and Marletta, M. A. (1994) *Methods Enzymol. 233*, 250−258.
59. Stone, J. R., Sands, R. H., Dunham, W. R., and Marletta, M. A. (1996) *Biochemistry 35*, 3258−3262.
60. Oertling, W. A., Kean, R. T., Wever, R., and Babcock, G. T. (1990) *Inorg. Chem. 29*, 2633−2645.
61. Tian, W. D., Sage, J. T., and Champion, P. M. (1993) *J. Mol. Biol. 233*, 155−166.

BI981547H